

Self-organized critical characteristics of TeV-photons from GRB 221009A

Wen-Long Zhang^{1,2}, Shuang-Xi Yi^{*1}, Yuan-Chuan Zou³, Fa-Yin Wang⁴, Cheng-Kui Li², and Sheng-Lun Xie⁵

¹ School of Physics and Physical Engineering, Qufu Normal University, Qufu 273165, China
e-mail: yisx2015@qfnu.edu.cn

² Key Laboratory of Particle Astrophysics, Institute of High Energy Physics, Chinese Academy of Sciences, Beijing 100049, China

³ School of Physics, Huazhong University of Science and Technology, Wuhan 430074, China
e-mail: zouyc@hust.edu.cn

⁴ School of Astronomy and Space Science, Nanjing University, Nanjing 210023, China ⁵ Institute of Astrophysics, Central China Normal University, Wuhan 430079, China

December 23, 2024

ABSTRACT

The very high-energy afterglow in GRB 221009A, known as the ‘Brightest Of All Time’ (B.O.A.T.), has been thoroughly analyzed in previous studies. In this paper, we conducted a statistical analysis of the waiting time behavior of 172 TeV photons from the B.O.A.T. observed by LHAASO-KM2A. The following results were obtained: (I) The waiting time distribution (WTD) of these photons deviates from the exponential distribution. (II) The behavior of these photons exhibits characteristics resembling those of a self-organized critical system, such as power-law distribution and scale-invariance features in the waiting time distribution. The power-law distribution of waiting times is consistent with the prediction of a non-stationary process. (III) The relationship between the power-law slopes of the WTD and the scale-invariant characteristics of the Tsallis q -Gaussian distribution deviates from existing theory. We suggest that this deviation is due to the photons not being completely independent of each other. In summary, the power-law and scale-free characteristics observed in these photons imply a self-organized critical process in the generation of TeV photons from GRB 221009A. Based on other relevant research, we propose that the involvement of a partially magnetically dominated component and the continuous energy injection from the central engine can lead to deviations in the generation of TeV afterglow from the simple external shock-dominated process, thereby exhibiting the self-organized critical characteristics mentioned above.

Key words. GRB 221009A; TeV-photons; SOC characteristic

1. Introduction

Gamma-ray bursts are sudden high-energy explosions in the cosmos, releasing a large amount of gamma-ray photons. Currently, there is no evidence of their occurrence within the Milky Way. Gamma-ray bursts mainly consist of two primary phases: prompt and multi-wavelength afterglow. The prompt phase is typically observed first when the gamma photon flux exceeds the threshold of high-energy photon monitoring satellites. Subsequently, other observation satellites are redirected to continuously monitor the potential multi-wavelength afterglow following the prompt phase. Multi-wavelength afterglow radiation spans a broad electromagnetic spectrum, including X-rays, radio, and optical bands, making it an indispensable tool for comprehensive gamma-ray burst research.

The use of imaging atmospheric Cherenkov telescopes (IACTs) has greatly broadened the energy limits of our observations of gamma-ray bursts, allowing us to see the ultra-high-energy radiation components from the universe, including the very high-energy (VHE) afterglow of gamma-ray bursts (MAGIC Collaboration et al. 2019a,b; Abdalla et al. 2019; H. E. S. S. Collaboration et al. 2021). In particular, the Large High Altitude Air-shower Observatory (LHAASO) has yielded numerous surprises, including the detection of VHE afterglow of the B.O.A.T. (“brightest of all time”) GRB 221009A (Burns et al. 2023; LHAASO Collaboration et al. 2023; Cao et al.

2023; Galanti et al. 2023) and the identification of the PeVatron (Lhaaso Collaboration 2024). The emission of TeV photons from the B.O.A.T. has been the subject of several studies, such as Jet Lorentz Factor (Gao & Zou 2023), Lorentz invariance violation (LIV) (Li & Ma 2023; Cao et al. 2024), MeV-TeV annihilation (Gao & Zou 2024) and dark matter candidate axion-like particles (ALP) (Carenza & Marsh 2022; Gao et al. 2024), while also providing a fresh perspective on our cognition. As mentioned by Gao & Zou (2024), some researchers have suggested that these TeV photons may originate from the prompt emission. And according to Wang et al. (2023) and Zhang et al. (2024), the TeV emission from the B.O.A.T. may reflect signatures of the prompt MeV emission. This leads us to speculate whether it is possible that each TeV photon is generated by a discrete event. If this is indeed the case, what connections exist between these events?

The concept of self-organized criticality (SOC) has been widely observed in various natural systems (Bak et al. 1988). It is also known as the “avalanche effect”. The primary manifestation of SOC systems is the power-law distribution of statistical parameters such as time and energy for multiple events, as well as the characteristic of scale invariance (Chang et al. 2017; Wei 2023). Systems ranging from sand piles to celestial bodies such as the Earth (Bak & Tang 1989; Caruso et al. 2007), the Sun (Wheatland 2000, 2003; Wang & Dai 2013; Peng et al. 2023), black holes (Wang & Dai 2017), soft gamma-ray repeaters (Cheng et al. 1996; Chang et al. 2017; Wang & Yu 2017;

Cheng et al. 2020; Zhang et al. 2023), some active galactic nuclei (Rees 1984; Yan et al. 2018) and high-mass X-ray binaries (Sidoli et al. 2019; Zhang et al. 2022), have exhibited the characteristics of self-organized critical systems in previous studies. Even in studies involving the prompt emission (Lyu et al. 2021; Li et al. 2023; Li & Yang 2023) and the X-ray or optical afterglows (Wang & Dai 2013; Yi et al. 2016, 2017) of gamma-ray bursts, as well as research on repeating fast radio bursts (Wang et al. 2023, 2024; Wu & Wang 2024), similar characteristics have been identified.

In the multi-band emission of gamma-ray bursts, the VHE radiation often displays relatively simple variability shapes, posing challenges in identifying SOC features using conventional methods. Fortunately, we have acquired TeV photon data detected by LHAASO and reconstructed by Cao et al. (2023). Section 2 presents the data source and the various analysis methods utilized. The findings from the data analysis are thoroughly discussed and analyzed in detail in section 3. Finally, our conclusions are presented in Section 4.

2. Data and Statistical analyses

On October 9, 2022, at 13:17:00.00 (denoted as T_0 hereafter), the Fermi Gamma-ray Burst Monitor (GBM) was triggered by an extraordinarily bright gamma-ray burst, GRB 221009A (Veres et al. 2022). At the same time, it also triggered several high-energy satellites such as Swift-BAT, Insight-HXMT, GECAM-C and Konus-Wind (Kennea et al. 2022; An et al. 2023; Frederiks et al. 2022). Subsequent optical observations determined the redshift of the GRB to be $z = 0.151$ (de Ugarte Postigo et al. 2022). LHAASO observed this GRB and detected more than 5000 VHE photons up to approximately 18 TeV, as reported by Huang et al. (2022). We collected data on the arrival times of 172 TeV photons from GRB 221009A detected by LHAASO-KM2A, as reported by Cao et al. (2023).

2.1. Waiting-time Distribution

The waiting time distribution (WTD) has become an important tool for us due to the unique nature of the obtained samples. In this section, we introduce the arrival time intervals of adjacent TeV-photons as waiting time, which is defined as $T_{\text{waiting}} = T_{i+1} - T_i$, where T_{i+1} and T_i are the arrival times for the $(i + 1)$ th and i th photon. We divide into two samples: one consisting of all 172 TeV photons, referred to as **Sample I**, and the other one consists of 143 TeV-photons arrived during the main emission time range of 230 s to 900 s (according to (Cao et al. 2023)), in order to take out possible background, referred to as **Sample II**.

Subsequently, we employ the exponential function, and thresholded power-law function to fit the distribution of waiting time. This is done to verify whether the overall process is generated by a completely random Poisson process and whether the distribution exhibits a power-law form. We then utilize the Tsallis q-Gaussian distribution (Tsallis et al. 1998) to investigate its scale invariance characteristics.

In this work, the python module *emcee*¹ is utilized to fit the data and get the confidence intervals of the parameters with the Monte Carlo Markov Chain (MCMC) method.

2.1.1. Exponential function

We first choose to fit the data distribution using an exponential function, which is expressed as follows:

$$f(x) \propto e^{-kx} \quad (1)$$

k and the amplitude are free parameters for this function, which need to be determined through fitting.

2.1.2. Thresholded Power-law function

In general, the differential distribution can be described by a thresholded power-law distribution (also called Generalized Pareto Type II distribution) with the following equation (Arnold 2008; Aschwanden 2015):

$$\frac{dN}{dx} \propto (x + x_0)^{-\alpha_x}, \quad (2)$$

The cumulative distribution can be expressed as the integral of the number of events exceeding a given value x . Therefore, the cumulative distribution function corresponding to Equation (2) can be expressed as ($\alpha_x \neq 1$):

$$N_{\text{cum}}(> x) = A + B \times (x + x_0)^{1-\alpha_x}, \quad (3)$$

where x_0 is a constant by considering the thresholded effects (e.g., incomplete sampling below x_0 , background contamination), α_x is the power-law slope of the distribution, N_{env} refers to the total number of events, x_1 and x_2 are the minimum and maximum values of x , respectively. The uncertainty of the cumulative distribution in a given bin i is approximately calculated as $\sigma_{\text{cum},i} = \sqrt{N_{\text{cum},i} - N_{\text{cum},i+1}}$ (Aschwanden 2019), where $N_{\text{cum},i}$ and $N_{\text{cum},i+1}$ is the number of events in the i th and $i + 1$ th bin.

The standard reduced chi-square (χ^2) goodness is used to identify the best fit. The χ can be written as

$$\chi_{\text{cum}} = \sqrt{\frac{1}{(n_x - n_{\text{par}})} \sum_{i=1}^{n_x} \frac{[N_{\text{cum},\text{th}}(x_i) - N_{\text{cum},\text{obs}}(x_i)]^2}{\sigma_{\text{cum},i}^2}} \quad (4)$$

for the cumulative distribution function (Aschwanden 2019), where n_x is the number of logarithmic bins, n_{par} is the number of the free parameters, $N_{\text{cum},\text{obs}}(x_i)$ is the observed values, $N_{\text{cum},\text{th}}(x_i)$ is the corresponding theoretical values for cumulative distribution, respectively.

2.2. Tsallis q-Gaussian Distribution

The Tsallis q-Gaussian distribution of waiting time is also a crucial tool for statistical research. Next, we will examine its application to the distribution of X_n , which is defined as $X_n = S_{i+n} - S_i$, where n is the temporal interval scale and S_i is the scale size of the i th waiting time. To reduce computation, we rescale X_n by σ_{X_n} as $x_n = X_n / \sigma_{X_n}$, where σ_{X_n} is the standard deviation of X_n . the differential distribution of x_n can be described with the function given by Tsallis et al. (1998) which can be written as

$$f(x_n) = A[1 - B(1 - q)x_n^2]^{1/(1-q)}, \quad (5)$$

the parameter of interest is q , while A and B represent free-fitting parameters.

¹ <https://pypi.org/project/emcee/>

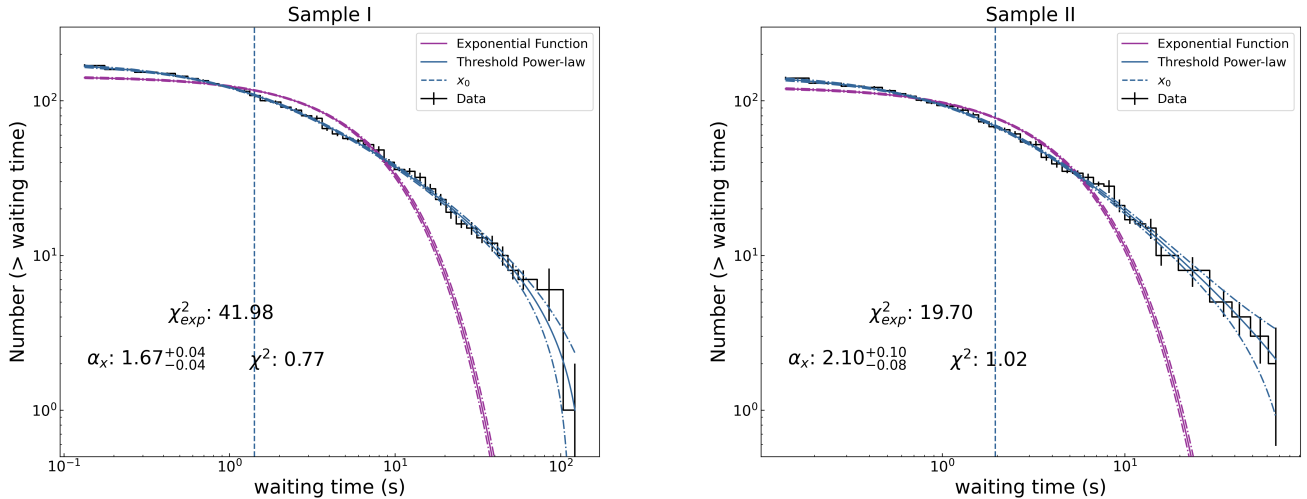


Fig. 1. Waiting time distributions and fitting results. The two panels depict the cumulative distributions of waiting time for **Sample I** and **Sample II**, which have been fitted with exponential (Eq. 1) and thresholded power-law (Eq. 3). The solid lines represent the best-fitting results for each function, while the regions between two dot-dashed lines indicate the 95% confidence level for each. Additionally, the dashed lines correspond to the thresholded values x_0 for the thresholded power-law.

It is worth mentioning that a theoretical relationship has been established between the power-law index α_x and the q value of the corresponding q -Gaussian, given by the equation (Celikoglu et al. 2010):

$$\alpha = \frac{2}{q-1}. \quad (6)$$

3. Fitting Results

3.1. Fitting Results of the WTD

The fitting results of the cumulative distributions of waiting times from Figure 1 clearly indicate that the WTD significantly deviates from the exponential distribution. The thresholded power-law fitting results of the cumulative distributions suggest that the WTD exhibits a pronounced power-law characteristic.

The fitting results for **Sample I** and **Sample II** yield $\alpha_x = 1.67^{+0.04}_{-0.04}$ and $\alpha_x = 2.10^{+0.10}_{-0.08}$, respectively, for their cumulative distributions. Here, α represents the power-law index of the thresholded power-law functions for each sample.

The fitting results of the distributions show a significant difference between the thresholded power-law and exponential fits. However, in the fitting of the distributions, the thresholded power-law function demonstrates better performance (with $\chi^2_{cum,I} = 0.77$ and $\chi^2_{cum,II} = 1.02$).

3.2. Tsallis q -Gaussian Distribution

After data reduction, it was found that both samples conform to the Tsallis q -Gaussian distribution. The left panel of Figure 2 shows examples of the probability density function for $n = 1, 5, 10, 20,$ and 50 , while the right panel illustrates the evolution of the fitting value of q over the range of n from 1 to 50. The fitting results illustrate that the distributions can be effectively fitted by the q -Gaussian function, and the value of q obtained

from the fitting remains relatively stable with variations in the value of n . The fitting results for **Sample I** and **Sample II** show $\bar{q}_I = 2.60^{+0.14}_{-0.14}$ and $\bar{q}_{II} = 2.53^{+0.14}_{-0.14}$, respectively.

4. Discussion

In terms of the distribution of waiting times, events generated by a Poisson process commonly exhibit an exponential distribution in their waiting times, especially for photons detected by the detector. However, the findings of this study suggest that the waiting time distribution of TeV photons detected by LHAASO deviates from the exponential distribution and aligns more closely with a power-law distribution. This indicates that these photons are not produced by independent Poisson processes for each event, suggesting a more intricate generation mechanism. Sahu et al. (2024) proposed that the VHE gamma-ray spectra of GRB 221009A observed by WCDA and KM2A at different time intervals and energy levels can be well elucidated using the photo-hadronic model, which includes extragalactic background light models. In this scenario, the generation of VHE photons is attributed to the interaction between high-energy protons and SSC photons in the forward shock region of the jet. Zhang et al. (2024) reveal a close relation between the keV-MeV and TeV emissions. The prompt emission in the keV-MeV band may continuously inject energy for the generation of TeV afterglow. Based on multi-wavelength and multi-messenger observations, Wang et al. (2023) discuss the constraints on the properties of gamma-ray burst ejecta, with the results favoring magnetic field dominance and suggesting the possibility of Poynting flux-dominated gamma-ray burst ejecta, as well as the potential for strong magnetic field dissipation and acceleration processes.

Based on our power-law fitting results, the self-organized criticality theory appears to offer a plausible explanation. According to the theoretical framework proposed by Aschwanden (2012), we can quantitatively link the concept of fractal dimensions in SOC avalanche systems to the power-law index of system parameters. The theory predicts that the power-law index of the distribution for SOC systems can be defined for Euclidean

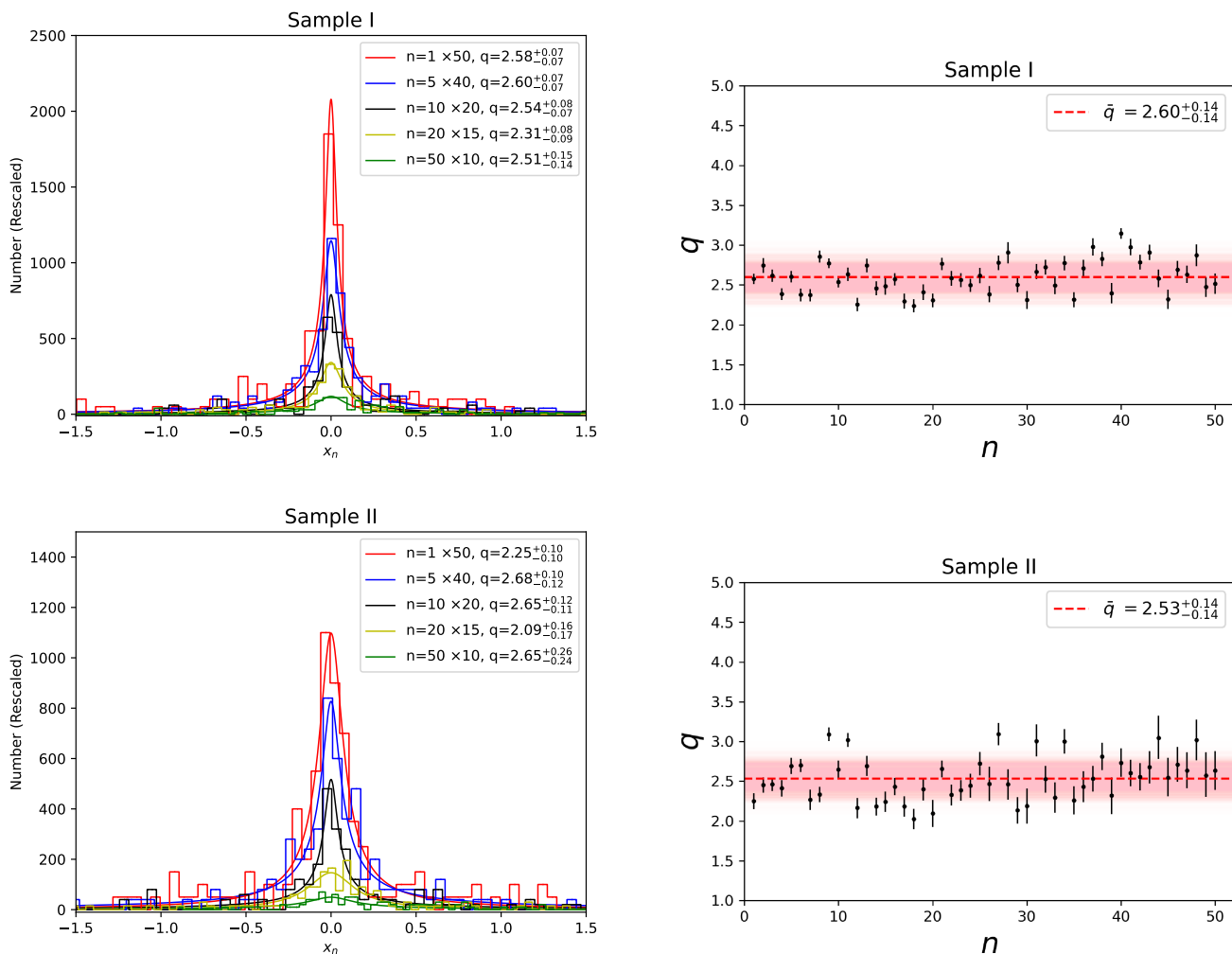


Fig. 2. Data (x_n) distributions and fitting results about q -Gauss. The left panel shows several examples of x_n distributions for different values of n and corresponding fitting curves (which are re-scaled to distinguish each sample). The right panel shows the evolutions between the best fitting results of q (with $1\text{-}\sigma$ error) and n of PDFs.

space dimensions $S = 1, 2, 3$. Aschwanden (2012) provides some theoretical indices, such as the duration frequency distribution (α_T), expressed as $\alpha_T = \frac{S+1}{2}$, where $S = 1, 2,$ and 3 represent the Euclidean dimensions. Specifically, theoretically, the slopes are $\alpha_T = 1, 1.5, 2$, for $S = 1, 2, 3$, respectively. Additionally, some studies have proposed that the generation of TeV photons may be associated with Poynting flux-dominated magnetic processes (Wang et al. 2023), thereby making the existence of a SOC process plausible. The power-law distribution is consistent with a non-stationary process, as discussed by Wheatland et al. (1998) and Aschwanden & McTiernan (2010). For instance, the interaction between external shocks and the circumstellar medium with a time-dependent rate.

The fitting results of the Tsallis q -Gaussian distribution reveal that the parameter q remains constant with the change of n and exhibits a certain scale invariance. However, this pattern significantly deviates from the theoretical relationship proposed by Celikoglu et al. (2010) as shown in Fig. (3), which we attribute to a generation mechanism that governs the occurrence of photon wait times, indicating a lack of independence and randomness. This inconsistency can be explained by contradicting the initial assumption in the derivation that the photons generated by the avalanche process are not completely Markovian (independent),

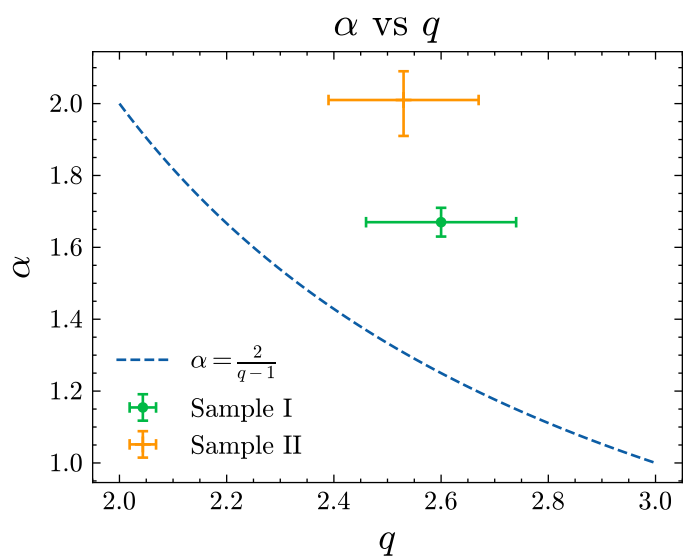


Fig. 3. The blue dashed line in the figure represents the relationship curve proposed by Celikoglu et al. (2010). The other data points correspond to the fitting results of two samples.

especially in **Sample II** with higher event rates, thus resulting in significant bias in this stage.

5. Conclusions

In this work, we investigate the behavior of TeV photons from the brightest gamma-ray burst GRB 221009A to date. We study the statistical properties of the waiting time of TeV photons using various methods. Our main conclusions are as follows:

(1). We find that dividing the waiting time of TeV photons into two samples, complete and partial, both exhibit well-defined power-law distributions in the cumulative distributions, significantly deviating from exponential distributions.

(2). After fitting the Tsallis q -Gaussian distribution to the fluctuations in the data, we observed that the parameter q exhibited a certain degree of constancy with respect to n , indicating a scale-invariance structure of avalanche size differences.

(3). The power-law index α_x and the scale invariance feature q exhibit deviations from the theoretical predictions, particularly in **Sample II**. We believe that this deviation indicates that the appearance of each TeV-photon is not completely random.

The most important conclusion is that, although power-law distributions and scale invariance features can serve as indicators of self-organized criticality (SOC), the deviation of the power-law index in **Sample II** from theoretical predictions suggest that this is not a typical self-organized critical process. The photons are not completely independent of each other, while still exhibiting fundamental characteristics of self-organized critical systems. We believe that this phenomenon may arise due to the energy injection from the central engine influencing the production of TeV radiation.

Acknowledgements. We thank the anonymous referee for thoughtful comments. We also thank Shao-Lin Xiong, Chen-Wei Wang, Wen-Jun Tan, Wang-Chen Xue and Yan-Qiu Zhang for helpful discussions. This work is supported by the National Natural Science Foundation of China (Grant Nos. 12494575, 12273009, U2038106, 12373047 and 12494575), the Natural Science Foundation of Jiangxi Province of China (grant No. 20242BAB26012) and the China Manned Space Project (CMS-CSST-2021-A12).

References

Abdalla, H., Adam, R., Aharonian, F., et al. 2019, *Nature*, 575, 464. doi:10.1038/s41586-019-1743-9

An, Z.-H., Antier, S., Bi, X.-Z., et al. 2023, arXiv:2303.01203. doi:10.48550/arXiv.2303.01203

Arnold, B. C. 2008, *Pareto and Generalized Pareto Distributions*, ed. D. Chotikapanich (New York, NY: Springer New York), 119–145, doi: 10.1007/978-0-387-72796-7_7

Aschwanden, M. J. 2012, *A&A*, 539, A2. doi:10.1051/0004-6361/201118237

Aschwanden, M. J. 2019, *ApJ*, 880, 105. doi:10.3847/1538-4357/ab29f4

Aschwanden, M. J. & McTiernan, J. M. 2010, *ApJ*, 717, 683. doi:10.1088/0004-637X/717/2/683

Aschwanden, M. J. 2015, *ApJ*, 814, 19. doi:10.1088/0004-637X/814/1/19

Bak, P. & Tang, C. 1989, *J. Geophys. Res.*, 94, 15, 635, 637. doi:10.1029/JB094iB11p15635

Bak, P., Tang, C., & Wiesenfeld, K. 1988, *Phys. Rev. A*, 38, 364. doi:10.1103/PhysRevA.38.364

Burns, E., Svinikin, D., Fenimore, E., et al. 2023, *ApJ*, 946, L31. doi:10.3847/2041-8213/acc39c

Cao, Z., Aharonian, F., Axikegu, B., et al. 2024, *Phys. Rev. Lett.*, 133, 071501. doi:10.1103/PhysRevLett.133.071501

Cao, Z., Aharonian, F., An, Q., et al. 2023, *Science Advances*, 9, ead72778. doi:10.1126/sciadv.ad72778

Carenza, P. & Marsh, M. C. D. 2022, arXiv:2211.02010. doi:10.48550/arXiv.2211.02010

Caruso, F., Pluchino, A., Latora, V., et al. 2007, *Phys. Rev. E*, 75, 055101. doi:10.1103/PhysRevE.75.055101

Celikoglu, A., Tirnakli, U., & Queirós, S. M. D. 2010, *Phys. Rev. E*, 82, 021124. doi:10.1103/PhysRevE.82.021124

Chang, Z., Lin, H.-N., Sang, Y., et al. 2017, *Chinese Physics C*, 41, 065104. doi:10.1088/1674-1137/41/6/065104

Cheng, B., Epstein, R. I., Guyer, R. A., et al. 1996, *Nature*, 382, 518. doi:10.1038/382518a0

Cheng, Y., Zhang, G. Q., & Wang, F. Y. 2020, *MNRAS*, 491, 1498. doi:10.1093/mnras/stz3085

de Ugarte Postigo, A., Izzo, L., Pugliese, G., et al. 2022, *GRB Coordinates Network, Circular Service*, No. 32648, 32648

Frederiks, D., Lysenko, A., Ridnaia, A., et al. 2022, *GRB Coordinates Network, Circular Service*, No. 32668, 32668

Galanti, G., Nava, L., Roncadelli, M., et al. 2023, *Phys. Rev. Lett.*, 131, 251001. doi:10.1103/PhysRevLett.131.251001

Gao, D.-Y. & Zou, Y.-C. 2024, *ApJ*, 961, L6. doi:10.3847/2041-8213/ad167d

Gao, D.-Y. & Zou, Y.-C. 2023, *ApJ*, 956, L38. doi:10.3847/2041-8213/acfd1

Gao, L.-Q., Bi, X.-J., Li, J., et al. 2024, *J. Cosmology Astropart. Phys.*, 2024, 026. doi:10.1088/1475-7516/2024/01/026

H. E. S. S. Collaboration, Abdalla, H., Aharonian, F., et al. 2021, *Science*, 372, 1081. doi:10.1126/science.abe8560

Huang, Y., Hu, S., Chen, S., et al. 2022, *GRB Coordinates Network, Circular Service*, No. 32677, 32677

Kennea, J. A., Williams, M., & Swift Team 2022, *GRB Coordinates Network, Circular Service*, No. 32635, 32635

LHAASO Collaboration, Cao, Z., Aharonian, F., et al. 2023, *Science*, 380, 1390. doi:10.1126/science.adg9328

Lhaaso Collaboration 2024, *Science Bulletin*, 69, 449. doi:10.1016/j.scib.2023.12.040

Li, H. & Ma, B.-Q. 2023, *J. Cosmology Astropart. Phys.*, 2023, 061. doi:10.1088/1475-7516/2023/10/061

Li, X.-J., Zhang, W.-L., Yi, S.-X., et al. 2023, *ApJS*, 265, 56. doi:10.3847/1538-4365/acc398

Li, X.-J. & Yang, Y.-P. 2023, *ApJ*, 955, L34. doi:10.3847/2041-8213/acf12c

Lyu, F., Li, Y.-P., Hou, S.-J., et al. 2021, *Frontiers of Physics*, 16, 14501. doi:10.1007/s11467-020-0989-x

MAGIC Collaboration, Acciari, V. A., Ansoldi, S., et al. 2019a, *Nature*, 575, 455. doi:10.1038/s41586-019-1750-x

MAGIC Collaboration, Acciari, V. A., Ansoldi, S., et al. 2019b, *Nature*, 575, 459. doi:10.1038/s41586-019-1754-6

Peng, F.-K., Wang, F.-Y., Shu, X.-W., et al. 2023, *MNRAS*, 518, 3959. doi:10.1093/mnras/stac3308

Rees, M. J. 1984, *ARA&A*, 22, 471. doi:10.1146/annurev.aa.22.090184.002351

Sahu, S., Medina-Carrillo, B., Páez-Sánchez, D. I., et al. 2024, *MNRAS*, 533, L64. doi:10.1093/mnras/slae063

Sidoli, L., Postnov, K. A., Belfiore, A., et al. 2019, *MNRAS*, 487, 420. doi:10.1093/mnras/stz1283

Tsallis, C., Mendes, R., & Plastino, A. R. 1998, *Physica A Statistical Mechanics and its Applications*, 261, 534. doi:10.1016/S0378-4371(98)00437-3

Veres, P., Burns, E., Bissaldi, E., et al. 2022, *GRB Coordinates Network, Circular Service*, No. 32636, 32636

Wang, F. Y. & Dai, Z. G. 2017, *MNRAS*, 470, 1101. doi:10.1093/mnras/stx1292

Wang, F. Y. & Dai, Z. G. 2013, *Nature Physics*, 9, 465. doi:10.1038/nphys2670

Wang, F. Y. & Yu, H. 2017, *J. Cosmology Astropart. Phys.*, 2017, 023. doi:10.1088/1475-7516/2017/03/023

Wang, F. Y., Wu, Q., & Dai, Z. G. 2023, *ApJ*, 949, L33. doi:10.3847/2041-8213/acd5d2

Wang, K., Tang, Q.-W., Zhang, Y.-Q., et al. 2023, arXiv:2310.11821. doi:10.48550/arXiv.2310.11821

Wang, K., Ma, Z.-P., Liu, R.-Y., et al. 2023, *Science China Physics, Mechanics, and Astronomy*, 66, 289511. doi:10.1007/s11433-023-2128-9

Wang, P., Song, L.-M., Xiong, S.-L., et al. 2024, *ApJ*, 975, 188. doi:10.3847/1538-4357/ad7de5

Wei, J.-J. 2023, *Physical Review Research*, 5, 013019. doi:10.1103/PhysRevResearch.5.013019

Wheatland, M. S., Sturrock, P. A., & McTiernan, J. M. 1998, *ApJ*, 509, 448. doi:10.1086/306492

Wheatland, M. S. 2000, *ApJ*, 536, L109. doi:10.1086/312739

Wheatland, M. S. 2003, *Sol. Phys.*, 214, 361. doi:10.1023/A:1024222511574

Wu, Q. & Wang, F.-Y. 2024, arXiv:2409.13247. doi:10.48550/arXiv.2409.13247

Yan, D., Wang, S., Zhang, P., et al. 2018, *ApJ*, 864, 164. doi:10.3847/1538-4357/aadd01

Yi, S.-X., Xi, S.-Q., Yu, H., et al. 2016, *ApJS*, 224, 20. doi:10.3847/0067-0049/224/2/20

Yi, S.-X., Yu, H., Wang, F. Y., et al. 2017, *ApJ*, 844, 79. doi:10.3847/1538-4357/aa7b7b

Zhang, W.-L., Li, X.-J., Yang, Y.-P., et al. 2023, *Research in Astronomy and Astrophysics*, 23, 115013. doi:10.1088/1674-4527/acf979

Zhang, W.-L., Yi, S.-X., Yang, Y.-P., et al. 2022, *Research in Astronomy and Astrophysics*, 22, 065012. doi:10.1088/1674-4527/ac6aac

Zhang, Y.-Q., Lin, H., Xiong, S.-L., et al. 2024, *ApJ*, 972, L25. doi:10.3847/2041-8213/ad6df8